Sulfurized-polyacrylonitrile in lithium-sulfur batteries: Interactions between undercoordinated carbons and polymer structure under low lithiation

Samuel Bertolini [a,*], Timo Jacob [a,b,c,*]

[a] Institute of Electrochemistry, Ulm University, Albert-Einstein-Allee 47, 89081 Ulm, Germany
[b] Helmholtz-Institute Ulm (HIU), Electrochemical Energy Storage, Helmholtzstr.11, 89081 Ulm, Germany
[c] Karlsruhe Institute of Technology (KIT), P.O. Box 3640, 76021 Karlsruhe, Germany

ARTICLE INFO

Keywords:
Density functional theory
Ab initio molecular dynamics
Lithium-sulfur batteries
Sulfurized-polyacrylonitrile

ABSTRACT

Lithium sulfur battery (LSB) represents an important candidate to be used in energy storage applications, due to its high specific capacities. Sulfurized polyacrylonitrile (SPAN) is a candidate as a host material in LSB to replace graphite, due to its ability to chemisorb polysulfides (PSs). The sulfur chains attached to the polymer can reversibly form Li_2S, and SPAN indicates to have a good cyclability and better performance than graphite, thus, SPAN acts partially as an active and also as a host material. In this study, we investigated the capacity of the solvent or the SPAN to lose a hydrogen atom from the backbone, to predict possible anodic reactions between solvent and host material. The simulation suggests that the phophilic salts may preferentially react with the solvent, and possibly building a cathode electrolyte interphase (CEI). We observed that an undercoordinated carbon (C_{uc}) can be thermodynamically created, due to lithiation. The C_{uc} can react with the solvent on the polymer backbone through different mechanisms, however, the simulations indicated that the reaction should be affected by the interaction between the solvent and C_{uc}, according to SPAN's configuration. Moreover, C_{uc} reacts with long sulfur chains attached to SPAN, capturing sulfur and forming a C S bond. A sulfur chain from one SPAN can connect to another polymer backbone, however, this process is affected by lithiation and vice versa. Therefore, this work also investigates the formation of interconnected SPAN structures and the multiple C_{uc} effects.

1. Introduction

Many different applications need energy storage devices, which normally use lithium ion batteries (LIBs) to convert chemical into electrical energy, such as electric vehicles, laptops, and solar panels [1,2]. However, there is an increasing demand for denser energy capacities and LSBs are promising candidates to replace LIBs, because LSBs have a theoretical specific capacity of 1672 mAh/g vs. 300 mAh/g of LIBs. Nevertheless, LSBs still have some challenges to overcome [3,4].

LSBs currently have a short life compared to LIBs, mainly due to the formation of polysulfides (PSs) or short circuits created by dendrites' growth in the anode. During cycling, the lithiation of the sulfur in the cathode produces intermediary PSs. Those PSs are soluble in the electrolyte (Li_2S_x, $3 \leq x \leq 8$) until the PSs can precipitate as a higher lithiated and insoluble salt (Li_2S_x, $x \leq 2$) [5 8]. Since the PSs are soluble in the electrolyte, they can shuttle between the electrodes and react with the Li metal anode, and irreversibly precipitate Li_2S in the anode surface. Therefore, the PSs can consume the anode, forming an insulator film, degrade the electrode due to volume expansion [9 11], and promote self discharge of the LSBs. In the positive electrode, the PSs can isolate the active material (sulfur) by covering it with a Li_2S layer or enclosing the porous of the host material (graphite), and not allowing the sulfur to be lithiated [12]. LSBs commonly use graphite as a host material, because sulfur does not conduct electricity. A common way to improve the cyclability of the LSBs is by modifying the architecture of the graphite to improve the PSs' lithiation in the cathode.

The architecture of the graphite changes the capacity of the LSBs. For e.g., carbon nanotube, graphite hollow spheres, graphite macro and microporous, all have different cyclability and capacities in a LSB, due to the capacity to retaining PSs in the cathode.

* Corresponding authors.
E-mail addresses: samuel.bertolini@alumni.uni-ulm.de (S. Bertolini), timo.jacob@uni-ulm.de (T. Jacob).

The shuttle of PSs to the anode can also be reduced by adding dopants or additives to the graphite. Those dopants and additives can adsorb PSs from the electrolyte, allowing further lithiation of the PSs [13 20]. Other strategies consist of covering the sulfur with a polymer that allows Li ion diffusion and consequently encapsulating the PSs inside the polymer or graphite [21 37]. Also, another alternative is to create an *in situ* solid electrolyte interphase (SEI) in the cathode. This SEI in the cathode is formed due to the reactions between the solvent and salt, where the salt removes H from the solvent in an environment with a depletion of electrons [38 41]. The attack of the salt on the solvent will allow the polymerization of the solvent in the cathode. Although the capacity of the LSBs using graphite as host materials can be improved by different methods, the interaction between the graphite and sulfur occurs through weak forces of van der Walls interactions.

One substitute of graphite as a host material is the SPAN, which indicates to improve the cyclability of the LSBs compared with graphite and also behaves as active material. Differently than in graphite, the interaction between the sulfur chains and the polymer backbone is through chemisorption [42 47]. SPAN is synthesized from polyacrylonitrile (PAN) and sulfur removes H from the polymer, producing H_2S. With the removal of the H from the polymer, π conjugated units are formed in the backbone, and the number of N C S units increases [48 51]. Moreover, the SPAN presents a conductive behavior due to the π conjugated units. Furthermore, the process presents the formation of 2 pyridylthiolates and thioamide, thus, we can assume a reasonable structure of the SPAN's backbone. The performance of the battery using SPAN can be affected by the temperature and sulfur content during syntheses. Moreover, the performance of the LSBs can be affected by the solvent composition and additives in the cathode that behave as sulfur [45,52,53].

In the literature, density functional theory (DFT) indicates that the longer is a sulfur chain, the more stable is the chain in the backbone. Also, when the sulfur chains increase, more stables are the ring like structures within the backbone [49]. Moreover, the lithiation of the sulfur chain suggests cleavage of the sulfur bond, and the energy to extract the PS from the polymer to the electrolyte is higher than 2 eV, however, the calculations were set without the presence of the solvent [50]. During the syntheses of SPAN, hydrogen can be removed from the cyclized polyacrylonitrile (cPAN) backbone without a sulfur chain being attached to the polymer, creating an C_{uc} in the polymer backbone. During vulcanization, the hydrogen removed from the polymer reacts with sulfur to produce hydrogen sulfide (H_2S) [54,55]. Also, a cleavage of C S bond during cycles suggests the formation of C_{uc} in the backbone. The change in the amount of the C S bonds observed by Archer et al. [56] corroborates with the assumption of the existence of C_{uc} in the backbone [56,57]. The solvent species affects the specific capacity of the LSBs using SPAN as host material [54,58]. Different structures of SPAN have been debated, including the sulfur chain being connected to different parts of the same polymer backbone or different polymer chains. Although polysulfide can be formed in SPAN, the material shows good cyclability and stability [51,54,59].

In our preview study [60], we observed that the PS, initially solvated in the electrolyte, can be captured by the polymer backbone, and the solvent can decompose in the presence of a C_{uc}. The capturing process occurs in the presence of a sulfur site SPAN and by a C_{uc}, i.e., cPAN missing a hydrogen termination. The capturing process can involve cleavage and recombination of S S bonds, the tendency is the PS forms a linear sulfur chain bonded to the cPAN. However, the presence of a salt, such as lithium bis(trifluoromethanesulfonyl)imide (LiTFSI), can affect the capturing process of the PS. The salt can increase the time for the sulfur chain to be completely reconstructed, increasing the lifetime of the sulfur fragments. Our studies also suggest that cPAN acts as an active material, and not only as a host material, as the polymer backbone can remove at least one Li ion from a PS. Experimental results proposed by Ming et al. suggest that nitrogen in cPAN can adsorb Li ion in place of sulfur [61]. Furthermore, cPAN within a C_{uc} can decompose the solvent, cleaving C O bound sulfur chains and producing a new ramification on the backbone.

This paper aims to investigate the effects of a new C_{uc} in the SPAN backbone, with the C_{uc} set around an absorbed PS. Also, we examined the reactions between the cPAN and the electrolyte, using all electrons basis set density functional methods (DFT) methods in the gas phase. We also studied the structure of the sulfur chain in the SPAN. This study illuminates how the SPAN structures can affect lithiation sulfur chains, and reveals new structures developed during cycles due to reactions between electrolyte and host material containing a C_{uc}. Additionally, this investigation elucidates that cleavage on C S during cycles may be affected by the lithiation, and consequently possible reactions between solvent and SPAN.

2. Computational methods

In this work, we used Vienna *Ab initio* Simulation Package (VASP) [62,63] code to perform the density functional theory calculations. The projector augmented wave (PAW) pseudopotentials and plane wave basis were set with an energy cut off of 400 eV to describe the electrons distribution [64,65]. Generalized gradient approximation (GGA) functional proposed by Perdew, Burke, and Ernzerhof (PBE) describes contributions from exchange and correlation energies. Van der Waals (vdW) dispersion corrections were included using the DFT D3 correction method of Grimme et al., including the damping formulation of Becke and Jonson [66,67]. *Ab initio* molecular dynamics (AIMD) simulations were carried out in the canonical ensemble (NVT) at 330 K, using a time step of 1 femtosecond and relaxing the ions through Velvet algorithm [68 70]. A Nosé mass parameter of 0.5 and Gaussian smearing with a width of 0.05 eV was used to calculate the effect of temperature. The charge analysis was performed using Bader calculations [71].

Some frames were selected from the AIMD to describe the different steps observed during the simulations. The energies of those single point frames obtained from the AIMD were calculated in such a way that the cPAN and the PS structure were kept rigid, while the electrolyte molecules were optimized. This procedure is motivated by the fact that we were mainly interested in the interaction between PS and cPAN. The optimization restricted to the solvent was used to minimize the effect of distortions on the solvents, created by the temperature, but maintaining the same solvation shell. Thus, changes in system's the total energy is mainly due to the reactions between PS and cPAN. All energies' evolution is concerning the initial configuration of the PS and cPAN as a reference, where the electrolyte was also optimized.

Before starting AIMD, the solvent molecules were kept rigid and van der Waals interactions were pre optimized by applying the consistent valence forcefield (cvff) [72]. Additionally, in this study longer sulfur chains (S_8 and S_6) were used to allow the possibility to form interconnected structures within the polymer backbone. Commonly a mixture of carbonates or ether based electrolytes are used together with SPAN [51,54,59]. We consider that, except reactions directly with 1,3 dioxolane (DOL), changing the solvent with another similar mixture would minimally affect the results, as they have similar solvation energies for Li ion and PS. Thus, in the present study, DOL was chosen as a pure solvent for simplification. Further investigation should take place to better understand the effect of the electrolyte when solvation structure considerably

changes, e.g., compare ether base, carbonate base, ionic liquids, and other solvents.

The geometry and electronic structures of the molecules in the gas phase model were optimized and studied in detail using the Gaussian09 (G09) package with the MP062X hybrid functional and an 6 311^{++}G (*d*, *p*) basis set [73 75]. The method was also used in the section Reactions in the gas phase.

2.1. C_{uc} sites in the same backbone

To sampling the Brillouin zone of C_{uc} sites in the same back bone, Monkhorst Pack method was used to mesh a 1 × 1 × 1 grid k points. Here, we investigated the interaction of an absorbed PS in the SPAN, and its interaction with a second C_{uc} in the same SPAN backbone, and we used the models shown in Fig. 1 to describe the system. The initial system was obtained from the preview papers [60], where the initial PSs were in the electrolyte, then, the PSs were captured by the cPAN, and the solvent surrounding the SPAN backbone is 1,3 dioxolane. We removed one H atom from the cPAN to create a new C_{uc} around the attached sulfur chain. Two different sized PSs were initially absorbed in cPAN, a S_6 chain, and a S_8 chain, together with 2Li ions absorbed on the backbone (origi nally part of a solvated polysulfide in the electrolyte) and already attached to the polymer backbone. One of the C_{uc} was set by removing the closest H atom of the sulfur chain (henceforth called close C_{uc}), while the other C_{uc} was set by removing the next H atom from SPAN (hereafter called jump C_{uc}). Model a.I and b.II (Fig. 1) used a close C_{uc} with different sulfur chains attached to SPAN, S_6, and S_8, respectively. In contrast, model b.I and b.II (Fig. 1) used a jump C_{uc} with different sulfur chains attached to SPAN, S_6 and S_8, respectively, as our interest was to evaluate if the sulfur chain can close ring structure in the backbone by attach ing to the C_{uc}.

2.2. A build up of interconnected backbones models and initial lithiation

In the interconnected backbones models, the Brillouin zone was set with a different grid, using the Monkhorst Pack method, the mesh was sampled with a 2 × 2 × 2 grid k points. The model is

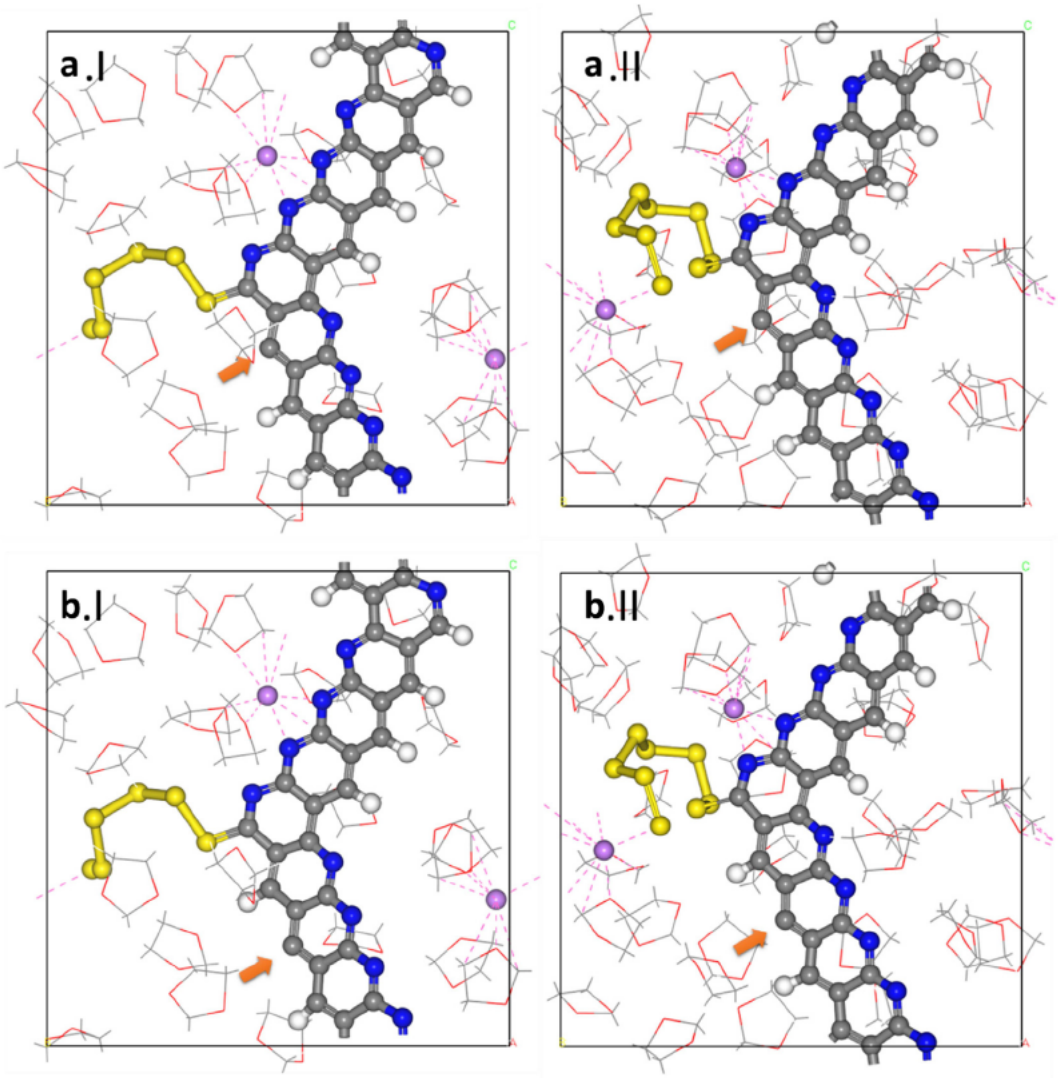

Fig. 1. The models describe a polysulfide initially adsorbed by a cyclized polyacrylonitrile. One Li-ion initially coordinates with the electrolyte and with sulfur in the edge of the sulfur chain, while the other Li-ion coordinates with the electrolyte, and with nitrogen in the polymer backbone. A new C_{uc} in the backbone is set around the sulfur chain: (a) the C_{uc} is set close to the sulfur chain (close-C_{uc}); (b) the C_{uc} is set after the next hydrogen termination (jump-C_{uc}); (I) the polysulfide absorbed was originally a Li_2S_6 solvated; and (II) the polysulfide absorbed was originally a Li_2S_8 solvated. Li-ions come originally from the polysulfide solvated in the electrolyte. The C_{uc} is indicated with an orange arrow. Carbon is set in gray, hydrogen in white, lithium in purple, nitrogen in blue, oxygen in red, and sulfur in yellow.

represented by two cPAN backbones. One backbone contains one Li and one sulfur chain (S_6) attached, while another backbone contains a C_{uc} (Fig. 2). A second Li is initially added to the system. In model a.1, this Li is added in the middle of the electrolyte as a solvated ion. In model b.1, the Li is added to the edge of the sulfur chain. After 10 ps of simulation, a third Li is added around the sulfur chain to each model (a.1 and b.1), which gives the structure of the models a.2 and b.2 (Fig. 2).

3. Results and discussion

3.1. Interactions between a second C_{uc} and an absorbed PS in the same backbone

Considering in SPAN that the same sulfur chain can be attached to the backbone in multiple carbon sites, the sulfur chain can have different sizes [48], and C_{uc} can exist during the synthesis and be produced during cycles [56,57]. We investigated the interaction of different PS in C_{uc} sites and the possibility to form a closed ring structure by forming a C S bond, without breaking a S S bond.

In the presence of a S_6 chain (models a.I and b.I), there is no exchange of S between C_{uc} and the sulfur attached to SPAN. This is an indication that small chains tend to not enclose their chain within the polymer backbone. Independent of the location of the C_{uc} and in the presence of a S_6 chain, the solvent will react with the C_{uc} and, therefore, the reaction between C_{uc} and DOL can occur in the presence of a close C_{uc} or jump C_{uc}. The process leading to the decomposition of the solvent is the same for both C_{uc} positions, as shown in Fig. 3 and Fig. S1. The decomposition process has as the first step of the reaction the approximation of one H atom from the solvent to the C_{uc}. The H close to the C_{uc} is located in the (CH_2) group of a DOL molecule. In the next step, the solvent donates this H atom to the C_{uc}. This reaction was observed around 13.90 ps of simulation, with a change in energy around 2.609 eV. Then, the C atom from DOL bounds to the backbone, where the C_{uc} previously was located after 15 ps of simulation, with the change in energy from the preview state of around 0.775 eV. A different decomposition process was observed in previous studies, where the DOL molecule breaks, forming a new ramification in the backbone [60]. However, the decomposition of the solvent was not observed in the presence of Li_2S_8. In the jump C_{uc}, and in presence of S_8 chain, we did not observe any reaction in the 15 ps of simu

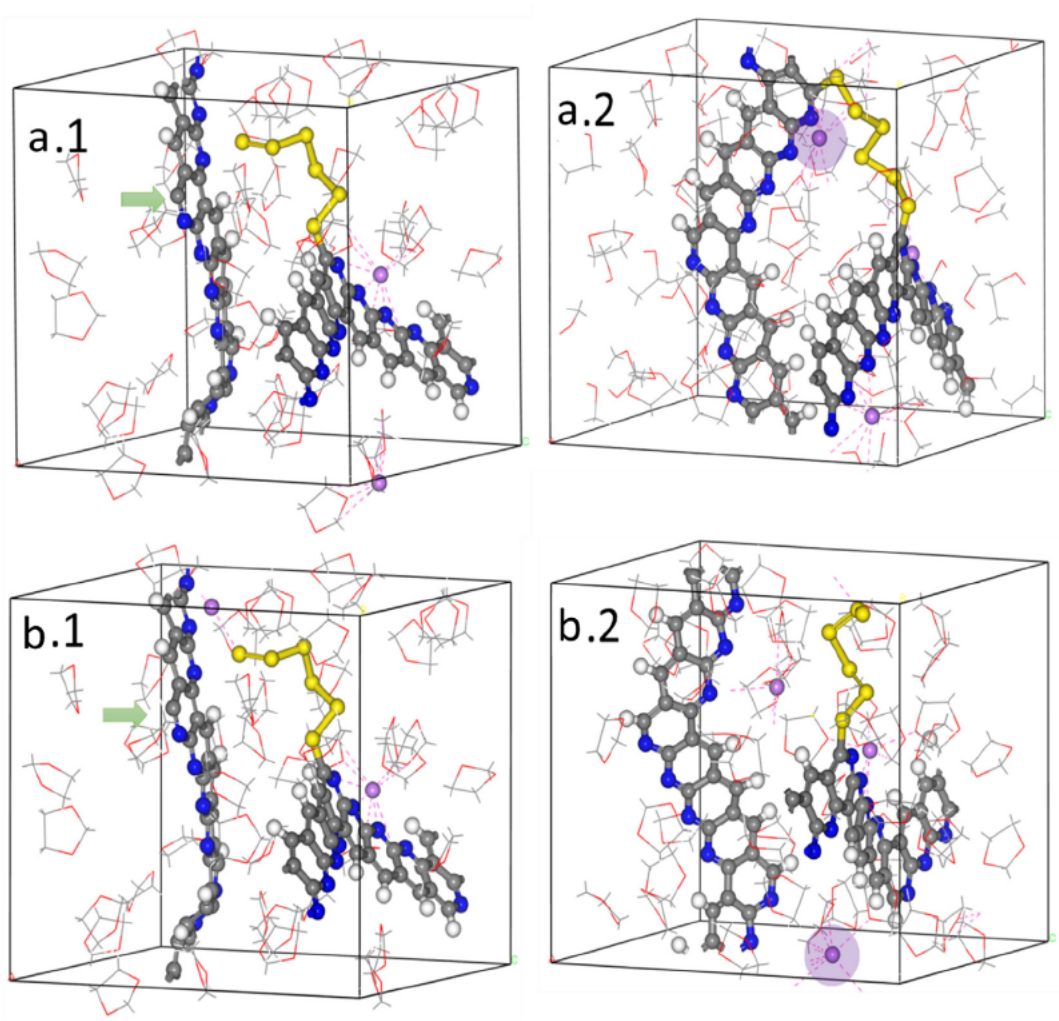

Fig. 2. The interconnected model interactions are built in two models. In both models, one of the cyclized polyacrylonitrile backbones contains an undercoordinated carbon indicated by a green arrow, while the other backbone contains one Li atom and one sulfur chain (S_6) attached to the polymer. In the model a.1, a second Li atom is dissolved in the electrolyte, but not close to the sulfur chain. In the model b.1, a second Li atom is dissolved in the electrolyte and closed of the sulfur chain. After 10 ps of simulation, another Li atom is added to the system, as highlighted in transparent purple, and set close to the sulfur chain; the models a.2 and b.2 are the lithiation of the models a.1 and b.1, respectively. Carbon is set in gray, hydrogen in white, lithium in purple, nitrogen in blue, oxygen in red, and sulfur in yellow.

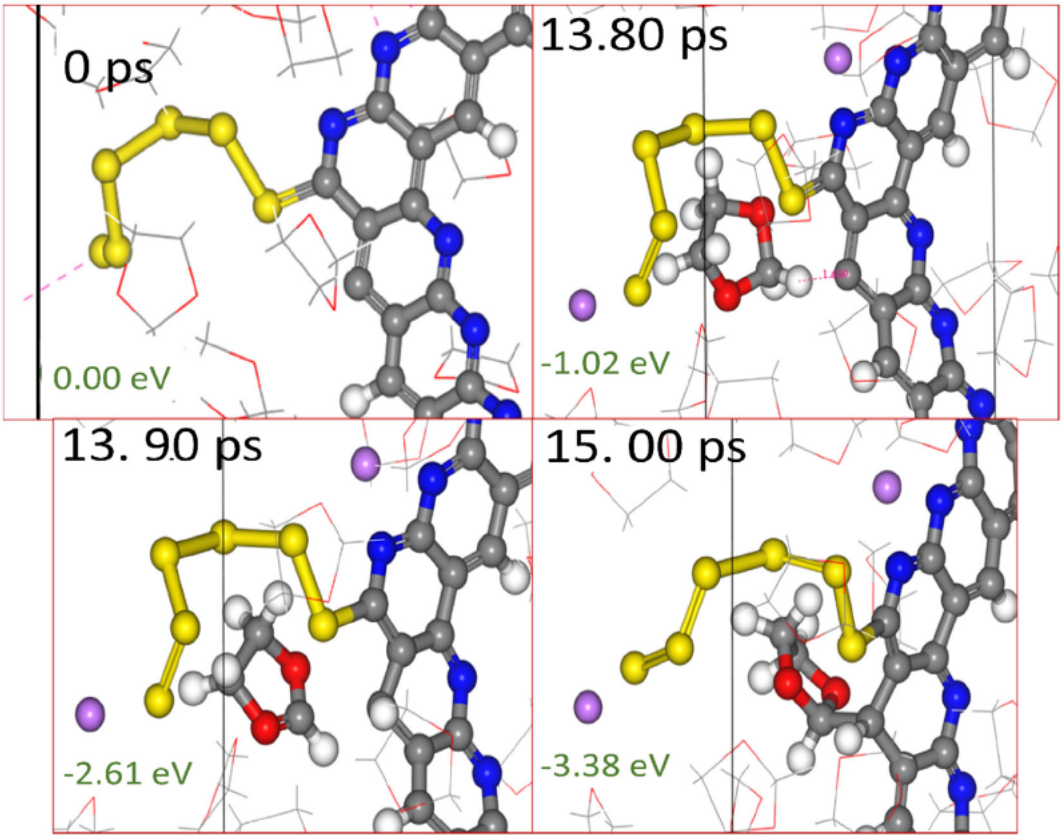

Fig. 3. Reaction between the solvent and the C_{uc}. Carbon is set in gray, hydrogen is white, lithium purple, nitrogen is blue, oxygen is red and sulfur is yellow.

lation (see Fig. S2). The reaction on the backbone may be related to the sulfur chains sized or a change in the configuration of the poly mer backbone. The simulations indicate that small chains (S_6) do not exchange sulfur between nearby C_{uc}, and C_{uc} tends to react with the solvent. The literature suggests that small sulfur chains can enclose the polymer backbone, and longer sulfur chains are more favorable to interconnect the polymer [48 51]. Although a closed ring structure with the polymer may form, e.g., during the synthesis, the lithiation would break the S S chains, creating par allel open chains structures with sulfur. Moreover, long chains reduce the kinetic for the solvent to react with C_{uc} or stop the reac tion. The simulation time was not enough to conclude that longer sulfur chains protect the C_{uc} against solvent decomposition, never theless, it is expected that the capacity of SPAN to decompose the solvent changes during cycles, due to change in the sulfur chain size, or capturing Li ions, or eliminating available C_{uc}. The effect of decomposed solvents on the polymer backbone, e.g., capturing Li ions or forming a cathode electrolyte interphase (CEI), is unknown and should be further investigated.

When the C_{uc} is set as close C_{uc} within a sulfur chain S_8 absorbed in the backbone (Fig. 4), the C_{uc} can remove S from the sulfur chain, forming a new C S bond. However, it also occurs a cleavage on a S S bond and a close ring structure formation is not observed. Initially, the sulfur chain is coordinated only by one Li ion, while the second Li ion was removed from the PS to coordinate with a N atom in the backbone. In the first step, after the new C_{uc} is set, a S S bond breaks to form a PS fragment, while the Li ion from the backbone is solvated back to connect both PS fragments created. As observed at 2.80 ps of simulation, this first step on the reaction changes the energy in around 1.059 eV. The first step indicates to be produced by the perturbation done by the creation of a C_{uc}, because on the second step, the system assumes a similar configuration as in the beginning. The second step takes place with 3.50 ps of simulation, with a small change in energy of 0.293 eV, comparing with the structure of the first step. Then the system assumes a similar configuration as at the begging of the simulation. On the next step, the C_{uc} captures one S from the sulfur chain, forming a fragment S_4 solvated in the elec trolyte and a fragment S_2 connecting both C_{uc}. This exchange of sulfur happens at 4.04 ps and indicates to be a metastable struc ture since the change in energy is around +0.221 eV. Continuous cleavage and rebound of the S S bonds allow different fragments to be solvated and also re captured by the backbone. For example, at time 7.82 ps of simulation, a continuous sulfur chain (S_8) is held by two different C_{uc}, while at 11.34 ps a fragment (LiS_6) is solvated in the electrolyte. However, the tendency is to form a S_7 coordinat ing with one Li ion and connected to the backbone, and the other C_{uc} is occupied by a single S atom. The C_{uc} occupied by a S atom may also be able to capture PS from the electrolyte. Therefore, the capability of the C_{uc} to capture solvated PS may be maintained. Thus, we would expect that here (Fig. 4), the single sulfur attached in the backbone continues to capture PSs from the electrolyte.

The charge of the different molecules in each system (sulfur chains, cPAN and DOL) has a small intensity oscillation over time around the average. Thus, the charge of the molecules can be con sidered constant over time, and this applies to all systems exam ined in this study. For example, the charge of the electrolyte is going to be neutral over time, and this can also occur when the sol vent decomposes and binds to the SPAN, or when the sulfur chain recombines in the SPAN. In the system that initially contains a C_{uc} close of a sulfur chain S_8, there is a small variation in the charge (~0.10 |e|) between cPAN and S_x, as shown in Fig. S5. Therefore, there is no considerable charge transference between the mole cules. However, this small charge oscillation between cPAN and the sulfur chains is dependent. Thus, when the charge of the cPAN increases, the charge of the sulfur chain decreases, and vice versa.

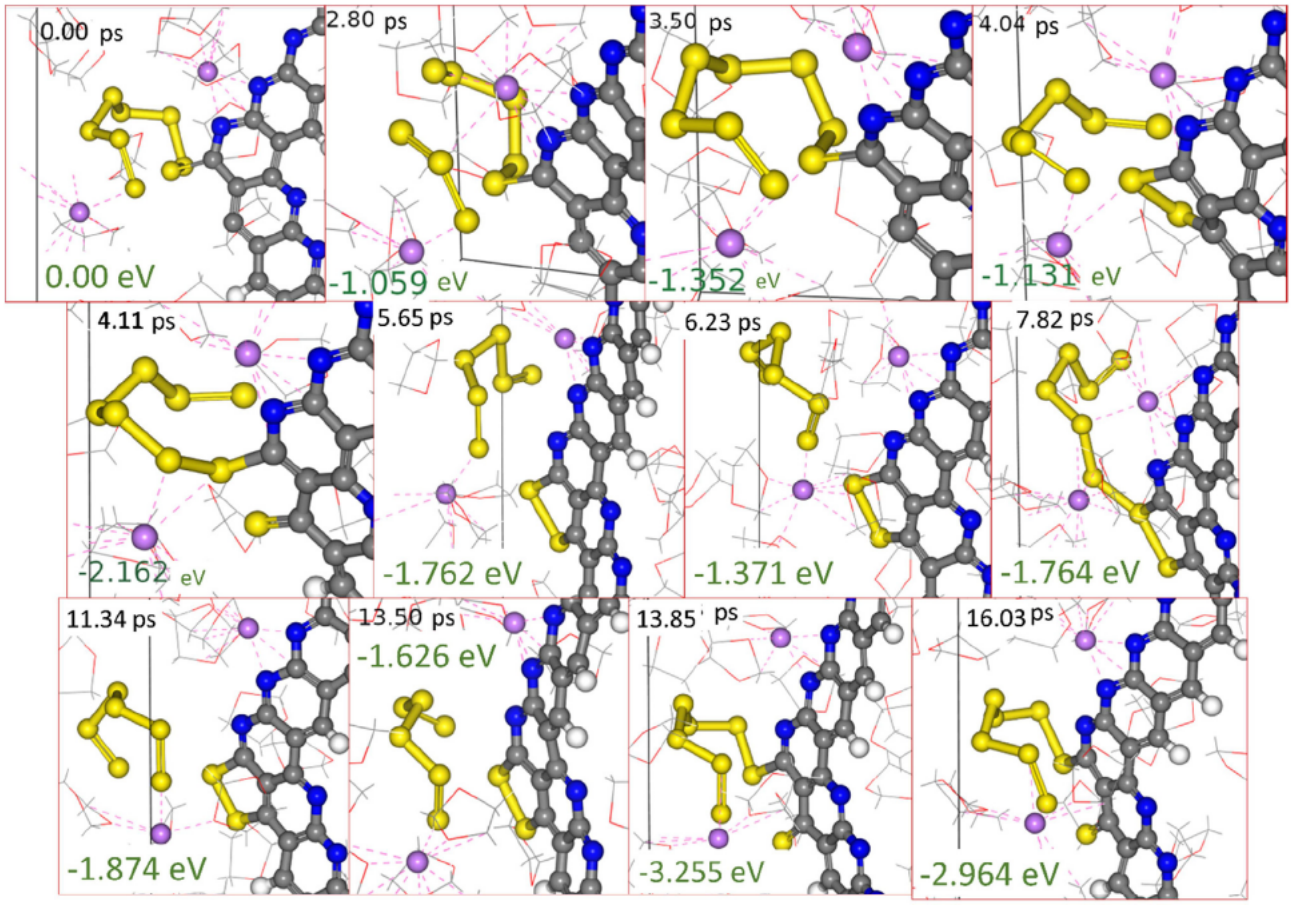

Fig. 4. The capturing process of sulfur from a sulfur chain to the C_{uc}. Carbon is set in gray, hydrogen is white, lithium purple, nitrogen is blue, oxygen is red and sulfur is yellow.

Therefore, the solvent only acts in the dissolution of sulfur fragments, while electrons move from the sulfur chain and the polymer backbone.

3.2. Interconnected backbones interactions and initial lithiation

When a second Li is not initially added to the system coordinating with the sulfur chain (model a.1 in Fig. 2), the C_{uc} can capture the sulfur chain from another backbone forming an interconnection between the backbones, connected by the same sulfur chain (Fig. 5). The interconnection remains even when a third Li is added to the system. A S S bond cleavage does not occur with the addition of a third Li surrounding the sulfur chain, indicating that this kind of structure should affect the charge and discharge process. Also, the third Li ion added around the sulfur chain moves to be completely solvated by DOL molecules, instead of reacting with the sulfur chain. We would expect that posteriorly, the Li ion should be captured by the backbone, since the polymer is able to remove Li ions from the PSs [60]. The simulation indicates that the structure proposed by Wang et al. [59] can be formed during

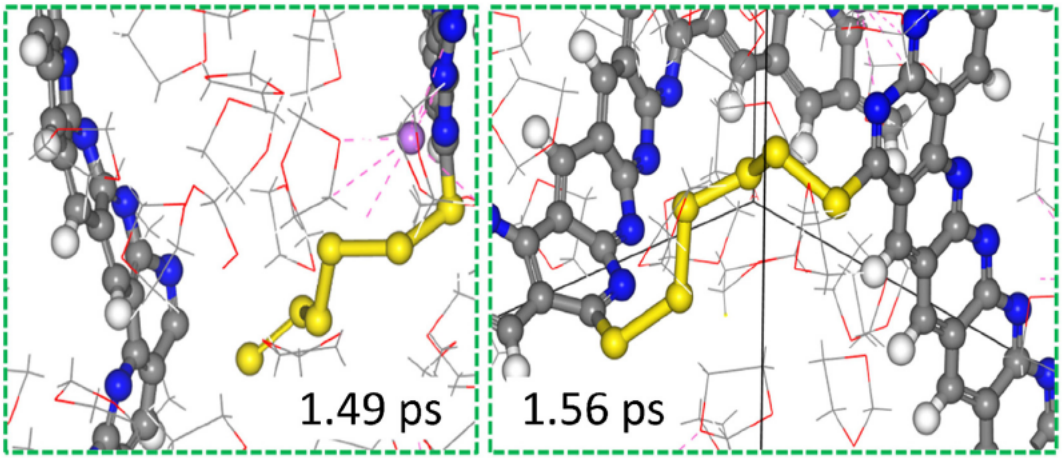

Fig. 5. Interconnection between two backbones forming during the simulation. Carbon is set in gray, hydrogen is white, lithium purple, nitrogen is blue, oxygen is red and sulfur is yellow.

charge and discharge, but also it may depend on the distribution and on the amount of Li ions on the positive electrode.

When a Li is set initially close to the sulfur chain, it does not allow the sulfur chain to connect between the polymer, consequently, the simulation indicates that lithiation will restrict the sulfur chain to create an interconnection between the polymer backbones. Although the location of the Li ion is important to the construction of the backbone interconnection, the general tendency is for the Li ions to be removed from the PS and be captured by the polymer [60]. Therefore, the propensity is to form the interconnection between different backbones. Nevertheless, when the Li ion is set on the edge of the PS and the interconnection does not happen, this exposes the C_{uc} to react with the solvent, as was observed in the simulation, but it will also allow that a new polysulfide can be captured by the C_{uc}, as observed in the previous studies [60]. Even though C_{uc} leans towards the decomposition of the solvent, as mentioned above, the decomposition of the DOL in presence of C_{uc} was not observed, when a sulfur chain (S_8) is attached to the polymer backbone. Additionally, further investigations should verify the effects of different solvents over the C_{uc}, although it is known that the solvent can affect the specific capacity of the battery [54,58].

The reaction between the solvent and the polymer (here observed) takes place with a different path to those reported in previous studies [60], in which the C_{uc} delivers a C O bond cleavage on the DOL molecule. Here, we observed a rupture on a C H bond, because H prefers to bound to C_{uc} than stay in the solvent (Fig. 6). Once DOL loses its weakest H atom (Fig. 6 and Fig. 8) to the polymer, the cleavage of two C O bonds is promoted. This will carry the formation of ethylene (CH_2CH_2) molecule and anomeric methine radical (OCHO). Another C O bond cleavage occurs in OCHO, liberating an O and formyl (HCO) radical. The O radical attacks on H from the polymer backbone, and then replaces the H atom by cleavage of the C H, and creating a H O and C O bond. The formyl radical (HCO) will supply a H atom to the sulfur chain attached to the polymer, breaking the sulfur chain and solvating it, together with the CO molecule created in the process. The simulations indicate that the solvent has an important role in the processes, closing C_{uc}, removing S atoms from the backbone, and reacting with the host material. Although reactivity of the C_{uc} tends to change with the amount of S and Li loaded in the backbone (as the simulations indicate), the use of different solvents beyond DOL has the potential to improve SPAN performance.

3.3. Reactions in the gas phase

We considered the presence of C_{uc}, possibly due to reactions during the synthesis of cPAN or the battery cycles and cleavage on the C S bonds during cycles [56,59]. Regarding a SPAN with a single S atom on the backbone being lithiated to form Li_2S and a C_{uc} ($cPAN^{e.s.}$, see Figs. 7 H5) as shown in Equation (1). The reaction is thermodynamically possible with a Gibbs free energy of 39.80 kcal/mol at 298 K. Therefore, new C_{uc} may be formed during cycles, and as mentioned above, the C_{uc} can be also be closed due to reactions with the solvent.

$$\mathrm{SPAN} + \frac{2}{9}\mathrm{Li_9} \quad \mathrm{cPAN^{e.s.}} + \mathrm{Li_2S}. \tag{1}$$

We used Equation (2) to analyze the Gibbs free energy to remove H atom from a molecule to form H_2, e.g., remove one H

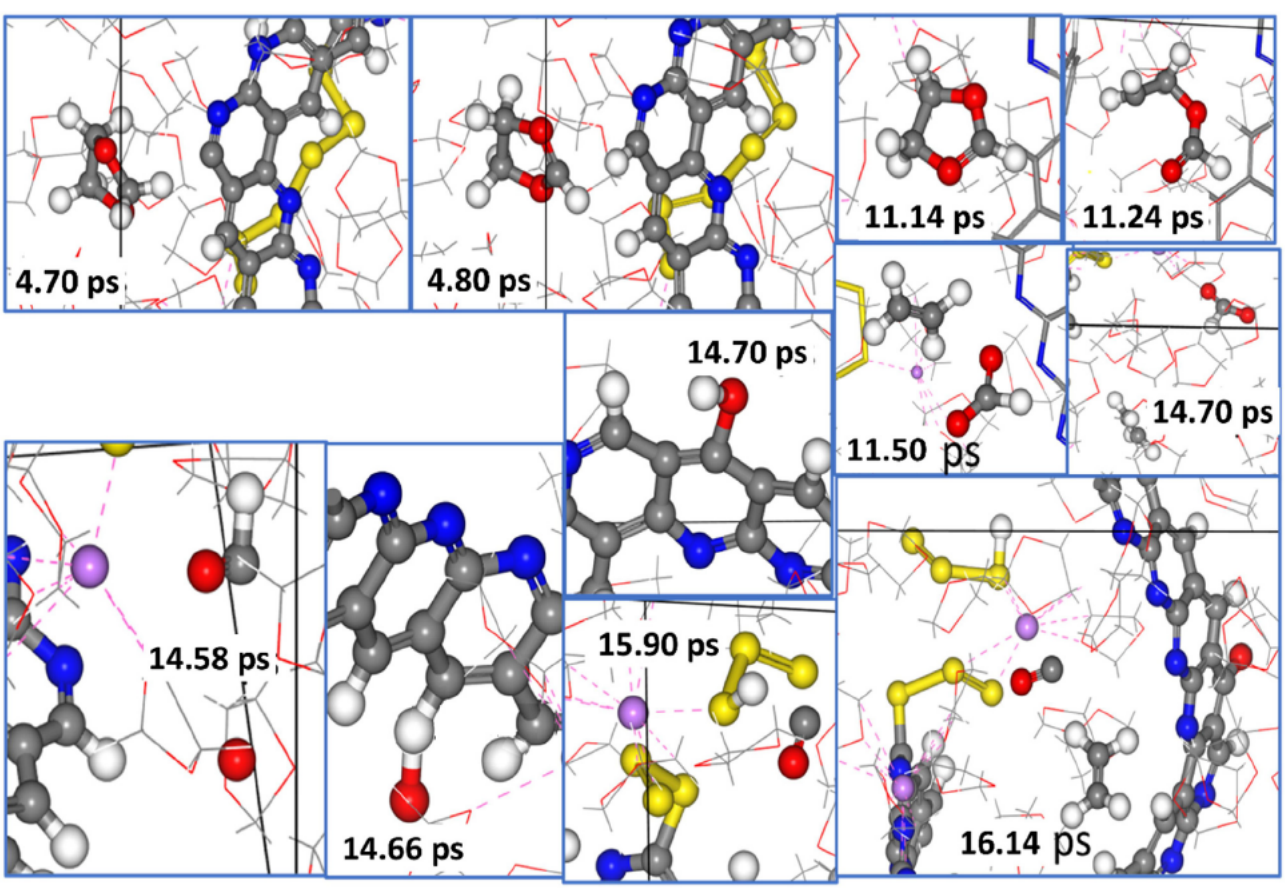

Fig. 6. Sequence of a solvent donating hydrogen to the backbone, posterior decomposing, and reacting with the polymer. Carbon is set in gray, hydrogen is white, lithium purple, nitrogen is blue, oxygen is red and sulfur is yellow.

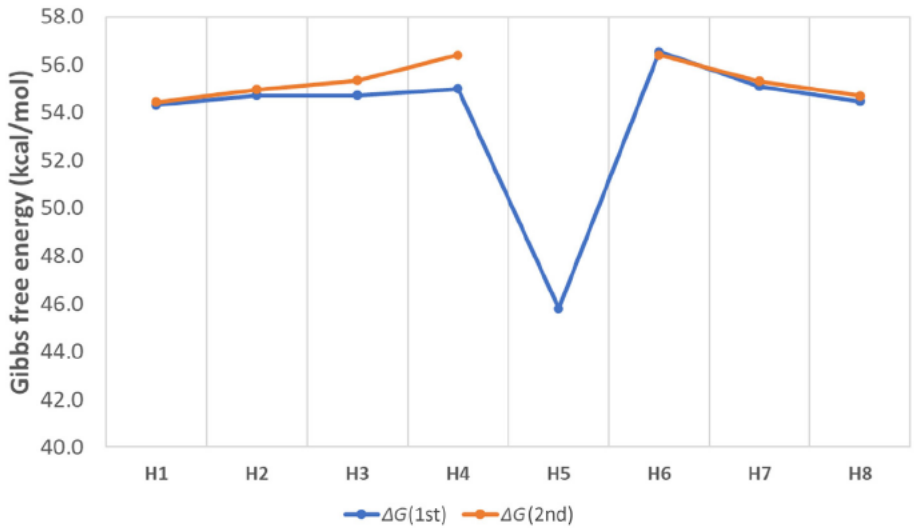

Fig. 7. Gibbs free energy (298 K) to extract H atoms from the cyclized-polyacrylonitrile producing a C_{uc} and H2, as described by Equation (2). Hydrogen is as a terminator on the backbone.

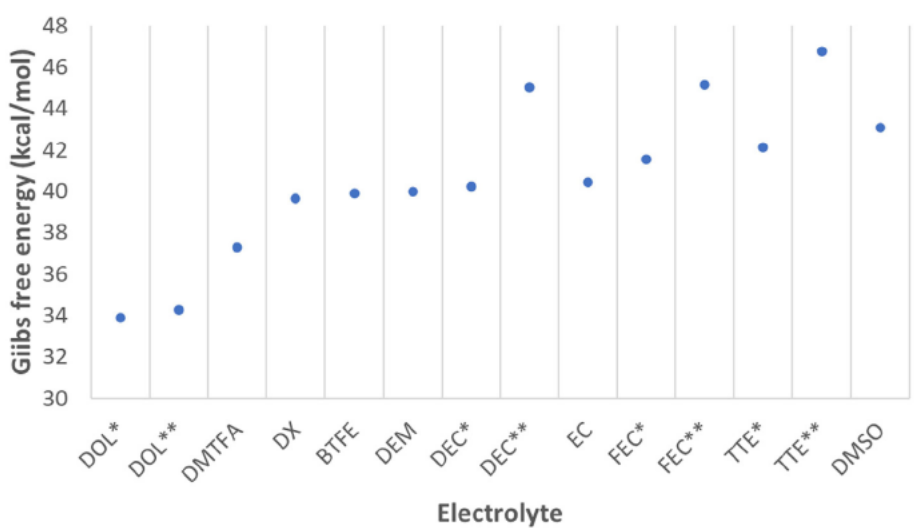

Fig. 8. Gibbs free energy (298 K) to extract H atoms from different electrolytes producing H_2, as described by Equation (2).

atom from the cPAN backbone to create an C_{uc}. As shown in Fig. 7, the termination H5 is the easiest to have H removed from the back bone (45.80 kcal/mol), and to create a C_{uc}. Moreover, the termina tion H5 is located in a region with a break in the symmetry, where the sequence of N atoms changes to a sequence of CH, and the lin ear configuration of cPAN changes direction. This indicates that the synthesis process during the transformation from PAN to cPAN may affect the performance of the battery, change the symmetry of cPAN backbone, and remove H atoms from the backbone.

The energy to remove the second hydrogen from the backbone is slightly higher than the one needed to remove the first hydrogen atom from the cPAN. The tendency, as shown in Fig. 7, is the energy necessary to remove H atoms from cPAN increases when the H is closer to the C_{uc}; e.g., the energy to remove H1 is 54.44 kcal/mol, and the energy to remove H4 is 56.40 kcal/mol. The small differ ence to remove H1 and H4 (1.96 kcal/mol) indicates that H atoms can be removed from the cPAN spread over the whole polymer extension. However, the simulation also suggests that the sulfur chains attached to the polymer backbone may be homogenized distributed.

$$A \quad \dot{A} + 0.5H_2. \tag{2}$$

During the battery cycles, Yushin et al. observed anodic reac tions with lithium bromide removing H atoms from the solvent, creating a CEI [38] in the cathode of lithium sulfur batteries. In this work, H_2 present in Equation (2) is used only as a reference for reaction equilibrium, it is not expected the formation of H_2 during cycles. Nevertheless, the use of additives such as LiBr or LiI may be able to anodic react with the hydrogen from the solvent [48 51]. We compared the Gibbs free energy ($\Delta G°$) at 298 K to remove a H atom from different solvents (Fig. 8) such as: 1,3 dioxolane; *n*, *n* dimethyltrifluoroacetamide (DMTFA); 1,4 Dioxane (DX); bis (2,2,2 trifluoroethyl) ether (BTFE); dimethoxyethane (DME); diethyl carbonate (DEC); ethylene carbonate (EC); fluoroethylene carbonate (FEC); 1,1,2,2 tetrafluoroethyl 2,2,3,3 tetrafluoropropyl ether (TTE); and dimethyl sulfoxide (DMSO).

For all the solvents calculated, the $\Delta G°$ to remove H atoms from the solvent is smaller than to remove H atoms from the cPAN. While in cPAN the minimal $\Delta G°$ value was 54.44 (remove 2nd H from cPAN), the maximum $\Delta G°$ in the solvent is 46.74 kcal/mol

(in TTE). Therefore, the calculations indicate that the cathode reac tions will preferentially remove H atoms from the solvents than from the cPAN. The effects of the solvents over a SPAN cathode, or salts that can remove H from the solvents (e.g., lithium bromide, LiBr) are still unclear, as several cathode reactions between an elec trolyte and SPAN occur. The effect of the electrolyte composition on the SPAN, or in the battery cyclability, might be further investi gated experimentally. However, the calculations indicated that sol vents, such as DOL (33.9 kcal/mol) can easier decompose, as compared with DMSO (43.1 kcal/mol). Phenomena, such as the for mation of CEI in the SPAN in the presence of LiBr, to block shuttle of polysulfide or creation of new C_{uc} should be correlated with the capacity to remove H atoms from the solvent. Additionally, we would expect the decomposition of the solvent and formation of CEI instead of the formation of C_{uc}.

The size of the PS dissolved in the electrolyte, as well as the size of the sulfur chain attached, affect the capacity of the polymer to capture a dissolved PS (see Fig. S6). Small PS chains (Li_2S_3) prefer entially dissolves in a longer sulfur chain attached to the polymer backbone. For example, the energy for Li_2S_3 to absorb in S_1.PAN is 43.35 kcal/mol and to absorb in S_5.PAN is 53.91 kcal/mol. The opposite is observed by longer polysulfide chains (Li_2S_4 and Li_2S_6), where the longer chains prefer to absorb in SPAN with a small chain on the backbone. Moreover, small PS chains (Li_2S_3) tend to be easier absorbed than longer PS chains (Li_2S_4 and Li_2S_6). The chain size of the PS tends to decrease with lithiation to form Li_2S, therefore, the simulations indicate a tendency for the adsorption capacity of SPAN to increase during lithiation.

4 Conclusion

In this study, we observed that in small chains (Li_2S_6), the sul fur chain attached to the SPAN does not exchange sulfur with nearby C_{uc} or form a close ring structure by bounding to the C_{uc}. However, the reactions with the solvent can take place, decomposing the solvent due to reactions with the C_{uc}. In con trast, long sulfur chains (Li_2S_8) can exchange sulfur when a C_{uc} is close enough to the sulfur chain attached to the SPAN back bone. Additionally, long sulfur chains indicate to improve stability of the C_{uc}, because during the 15 ps of simulation no reactions have been observed between C_{uc} and DOL. Moreover, the inter connection between different polymer backbones is possible, but it is affected by lithiation.

The energy to remove the first hydrogen from cPAN is approx imately 54.5 kcal/mol, where the weakest H atom is located in an asymmetric position on the polymer backbone. To remove a second hydrogen, the energy increases to around 56.5 kcal/mol, and it is easier to remove H atoms that are not nearby the first C_{uc}. Moreover, it is easier to remove H atoms from a solvent than from the polymer, which indicates that a possible anodic reaction first decomposes the solvent (e.g., reaction with LiBr as additive).

The absorption of small PS chains (Li_2S_3) tends to be stronger than long chains (Li_2S_4 and Li_2S_6). Additionally, Li_2S_3 prefers to absorb in longer chains, while Li_2S_4 and Li_2S_6 tend to absorb in smaller sulfur chains attached to the SPAN. The observation sug gests that the capacity of SPAN to capture PS could change during cycles, depending on the concentration of each fragment dissolved in the electrolyte.

Declaration of Competing Interest

The authors declare that they have no known competing finan cial interests or personal relationships that could have appeared to influence the work reported in this paper.

Acknowledgments

Support from the Deutsche Forschungsgemeinschaft (DFG) through Project ID 390874152 (POLiS Cluster of Excellence) as well as the Schwerpunktprogramm (priority program) SPP 2248 (polymer based batteries) is gratefully acknowledged. The authors also acknowledge the computer time supported by the state of Baden Württemberg through the HPC project 511 and the Deutsche Forschungsgemeinschaft (DFG) through Grant Number INST40/467 1 FUGG.

Appendix A. Supplementary data

Supplementary data to this article can be found online at https://doi.org/10.1016/j.jechem.2021.08.070.

References

[1] E.P. Kamphaus, S. Angarita-Gomez, X. Qin, M. Shao, P.B. Balbuena, ChemPhysChem 21 (2020) 1310–1317.
[2] A. Marzouk, V. Ponce, L. Benitez, F.A. Soto, K. Hankins, J.M. Seminario, P.B. Balbuena, F. El-Mellouhi, J. Phys. Chem. C 122 (2018) 25858–25868.
[3] S. Sharifi-Asl, F.A. Soto, T. Foroozan, M. Asadi, Y. Yuan, R. Deivanayagam, R. Rojaee, B. Song, X. Bi, K. Amine, J. Lu, A. Salehi-khojin, P.B. Balbuena, R. Shahbazian-Yassar, Adv. Funct. Mater. 29 (2019) 1901110.
[4] Y. Zheng, F.A. Soto, V. Ponce, J.M. Seminario, X. Cao, J.-G. Zhang, P.B. Balbuena, J. Mater. Chem. A 7 (2019) 25047–25055.
[5] Y.-X. Chen, P. Kaghazchi, Nanoscale 6 (2014) 13391–13395.
[6] Y. Yang, G. Zheng, Y. Cui, Chem. Soc. Rev. 42 (2013) 3018–3032.
[7] H. Schneider, C. Gollub, T. Weiß, J. Kulisch, K. Leitner, R. Schmidt, M.M. Safont-Sempere, Y. Mikhaylik, T. Kelley, C. Scordilis-Kelley, J. Electrochem. Soc. 161 (2014) A1399.
[8] A.F. Hofmann, D.N. Fronczek, W.G. Bessler, J. Power Sources 259 (2014) 300–310.
[9] L. Yuan, X. Qiu, L. Chen, W. Zhu, J. Power Sources 189 (2009) 127–132.
[10] C. Barchasz, J.-C. Leprêtre, F. Alloin, S. Patoux, J. Power Sources 199 (2012) 322–330.
[11] Y. Yang, G. Zheng, S. Misra, J. Nelson, M.F. Toney, Y. Cui, J. Am. Chem. Soc. 134 (2012) 15387–15394.
[12] J.C. Burgos, P.B. Balbuena, J. Phys. Chem. C 117 (2013) 4639–4646.
[13] M.-S. Song, S.-C. Han, H.-S. Kim, J.-H. Kim, K.-T. Kim, Y.-M. Kang, H.-J. Ahn, S. Dou, J.-Y. Lee, J. Electrochem. Soc. 151 (2004) A791.
[14] Y. Zhang, Y. Zhao, A. Yermukhambetova, Z. Bakenov, P. Chen, J. Mater. Chem. A 1 (2013) 295–301.
[15] Y. Choi, B. Jung, D. Lee, J. Jeong, K. Kim, H. Ahn, K. Cho, H. Gu, Phys. Scr. 2007 (2007) 62.
[16] X. Ji, S. Evers, R. Black, L.F. Nazar, Nat. Commun. 2 (2011) 1–7.
[17] S. Evers, T. Yim, L.F. Nazar, J. Phys. Chem. C 116 (2012) 19653–19658.
[18] J. Song, M.L. Gordin, T. Xu, S. Chen, Z. Yu, H. Sohn, J. Lu, Y. Ren, Y. Duan, D. Wang, Angew. Chem. Int. 127 (2015) 4399–4403.
[19] K. Han, J. Shen, S. Hao, H. Ye, C. Wolverton, M.C. Kung, H.H. Kung, ChemSusChem 7 (2014) 2545–2553.
[20] J. Balach, T. Jaumann, M. Klose, S. Oswald, J. Eckert, L. Giebeler, J. Power Sources 303 (2016) 317–324.
[21] Y. Yang, G. Yu, J.J. Cha, H. Wu, M. Vosgueritchian, Y. Yao, Z. Bao, Y. Cui, ACS Nano 5 (2011) 9187–9193.
[22] W. Li, G. Zheng, Y. Yang, Z.W. Seh, N. Liu, Y. Cui, Proc. Natl. Acad. Sci. 110 (2013) 7148–7153.
[23] B. Zhang, X. Qin, G. Li, X. Gao, Energy Environ. Sci. 3 (2010) 1531–1537.
[24] X. Li, Y. Cao, W. Qi, L.V. Saraf, J. Xiao, Z. Nie, J. Mietek, J.-G. Zhang, B. Schwenzer, J. Liu, J. Mater. Chem. 21 (2011) 16603–16610.
[25] C. Liang, N.J. Dudney, J.Y. Howe, Chem. Mater. 21 (2009) 4724–4730.
[26] W. Zheng, Y. Liu, X. Hu, C. Zhang, Electrochim. Acta 51 (2006) 1330–1335.
[27] Y.-S. Su, Y. Fu, A. Manthiram, Phys. Chem. Chem. Phys. 14 (2012) 14495–14499.
[28] A. Manthiram, Y.-S. Su, Google Patents (2015).
[29] G. Zheng, Y. Yang, J.J. Cha, S.S. Hong, Y. Cui, Nano Lett. 11 (2011) 4462–4467.
[30] L. Ji, M. Rao, S. Aloni, L. Wang, E.J. Cairns, Y. Zhang, Energy Environ. Sci. 4 (2011) 5053–5059.
[31] J. Guo, Y. Xu, C. Wang, Nano Lett. 11 (2011) 4288–4294.
[32] H. Ye, Y.-X. Yin, S. Xin, Y.-G. Guo, J. Mater. Chem. A 1 (2013) 6602–6608.
[33] X. Tao, X. Chen, Y. Xia, H. Huang, Y. Gan, R. Wu, F. Chen, J. Mater. Chem. A 1 (2013) 3295–3301.
[34] S. Wei, H. Zhang, Y. Huang, W. Wang, Y. Xia, Z. Yu, Energy Environ. Sci. 4 (2011) 736–740.
[35] B. Zhang, C. Lai, Z. Zhou, X. Gao, Electrochim. Acta 54 (2009) 3708–3713.
[36] N. Jayaprakash, J. Shen, S.S. Moganty, A. Corona, L.A. Archer, Angew. Chem. Int. 50 (2011) 5904–5908.
[37] L. Yuan, H. Yuan, X. Qiu, L. Chen, W. Zhu, J. Power Sources 189 (2009) 1141–1146.

[38] F. Wu, S. Thieme, A. Ramanujapuram, E. Zhao, C. Weller, H. Althues, S. Kaskel, O. Borodin, G. Yushin, Nano Energy 40 (2017) 170–179.
[39] O. Borodin, W. Behl, T.R. Jow, J. Phys. Chem. C 117 (2013) 8661–8682.
[40] H. Kim, F. Wu, J.T. Lee, N. Nitta, H.T. Lin, M. Oschatz, W.I. Cho, S. Kaskel, O. Borodin, G. Yushin, Adv. Energy Mater. 5 (2015) 1401792.
[41] F. Wu, J.T. Lee, N. Nitta, H. Kim, O. Borodin, G. Yushin, Adv. Mater. 27 (2015) 101–108.
[42] S.-C. Zhang, L. Zhang, W.-K. Wang, W.-J. Xue, Synth. Met. 160 (2010) 2041–2044.
[43] L. Xiao, Y. Cao, J. Xiao, B. Schwenzer, M.H. Engelhard, L.V. Saraf, Z. Nie, G.J. Exarhos, J. Liu, Adv. Mater. 24 (2012) 1176–1181.
[44] J. Wang, J. Yang, J. Xie, N. Xu, Adv. Mater. 14 (2002) 963–965.
[45] Y. Zhang, S. Liu, G. Li, G. Li, X. Gao, J. Mater. Chem. A 2 (2014) 4652–4659.
[46] H. Peng, X. Wang, Y. Zhao, T. Tan, A. Mentbayeva, Z. Bakenov, Y. Zhang, J. Nanoparticle Res. 19 (2017) 1–8.
[47] J. Li, K. Li, M. Li, D. Gosselink, Y. Zhang, P. Chen, J. Power Sources 252 (2014) 107–112.
[48] J. Fanous, M. Wegner, J. Grimminger, A.n. Andresen, M.R. Buchmeiser, Chem. Mater. 23 (2011) 5024–5028.
[49] T. Zhu, J.E. Mueller, M. Hanauer, U. Sauter, T. Jacob, ChemElectroChem 4 (2017) 2494–2499.
[50] T. Zhu, J.E. Mueller, M. Hanauer, U. Sauter, T. Jacob, ChemElectroChem 4 (2017) 2975–2980.
[51] M. Frey, R.K. Zenn, S. Warneke, K. Müller, A. Hintennach, R.E. Dinnebier, M.R. Buchmeiser, ACS Energy Lett. 2 (2017) 595–604.
[52] L. Wang, X. He, J. Li, M. Chen, J. Gao, C. Jiang, Electrochim. Acta 72 (2012) 114–119.
[53] W.J. Chen, B.Q. Li, C.X. Zhao, M. Zhao, T.Q. Yuan, R.C. Sun, J.Q. Huang, Q. Zhang, Angew. Chem. Int. 59 (2020) 10732–10745.
[54] S.S. Zhang, Energies 7 (2014) 4588–4600.
[55] J. Ye, F. He, J. Nie, Y. Cao, H. Yang, X. Ai, J. Mater. Chem. A 3 (2015) 7406–7412.
[56] S. Wei, L. Ma, K.E. Hendrickson, Z. Tu, L.A. Archer, J. Am. Chem. Soc. 137 (2015) 12143–12152.
[57] T.N.L. Doan, M. Ghaznavi, Y. Zhao, Y. Zhang, A. Konarov, M. Sadhu, R. Tangirala, P. Chen, J. Power Sources 241 (2013) 61–69.
[58] S. Warneke, A. Hintennach, M.R. Buchmeiser, J. Electrochem. Soc. 165 (2018) A2093.
[59] X. Wang, Y. Qian, L. Wang, H. Yang, H. Li, Y. Zhao, T. Liu, Adv. Funct. Mater. 29 (2019) 1902929.
[60] S. Bertolini, T. Jacob, ACS Omega 6 (2021) 9700–9708.
[61] W. Wang, Z. Cao, G.A. Elia, Y. Wu, W. Wahyudi, E. Abou-Hamad, A.-H. Emwas, L. Cavallo, L.-J. Li, J. Ming, ACS Energy Lett. 3 (2018) 2899–2907.
[62] G. Kresse, J. Hafner, Phys. Rev. B 48 (1993) 13115.
[63] G. Kresse, J. Furthmüller, Phys. Rev. B 54 (1996) 11169–11186.
[64] P.E. Blöchl, Phys. Rev. B 50 (1994) 17953–17979.
[65] G. Kresse, D. Joubert, Phys. Rev. B 59 (1999) 1758–1775.
[66] S. Grimme, S. Ehrlich, L. Goerigk, J. Comput. Chem. 32 (2011) 1456–1465.
[67] S. Grimme, J. Antony, S. Ehrlich, H. Krieg, J. Chem. Phys. 132 (2010) 154104.
[68] S. Nosé, J. Chem. Phys. 81 (1984) 511–519.
[69] N. Shuichi, Prog. Theor. Phys. Supp. 103 (1991) 1–46.
[70] D. Bylander, L. Kleinman, Phys. Rev. B 46 (1992) 13756.
[71] A. Arnaldsson Henkelman, H. Jónsson, Comput. Mater. Sci. 36 (2006) 254–360.
[72] P. Dauber-Osguthorpe, V.A. Roberts, D.J. Osguthorpe, J. Wolff, M. Genest, A.T. Hagler, Proteins: Struct., Funct., Genet. 4 (1988) 31–47.
[73] M.J. Frisch, G.W. Trucks, H.B. Schlegel, G.E. Scuseria, M.A. Robb, J.R. Cheeseman, G. Scalmani, V. Barone, G.A. Petersson, H. Nakatsuji, X. Li, M. Caricato, A.V. Marenich, J. Bloino, B.G. Janesko, R. Gomperts, B. Mennucci, D.J. Hratch, Gaussian, 16, Gaussian, Inc, Wallingford, CT, 2016.
[74] A.D. Beck, J. Chem. Phys 98 (1993) 5648–15646.
[75] J.P. Perdew, J.A. Chevary, S.H. Vosko, K.A. Jackson, M.R. Pederson, D.J. Singh, C. Fiolhais, Phys. Rev. B 46 (1992) 6671.